Neuroscience 177 (2011) 252–268

MORPHOLOGICAL AND ELECTROPHYSIOLOGICAL PROPERTIES OF PYRAMIDAL-LIKE NEURONS IN THE STRATUM ORIENS OF CORNU AMMONIS 1 AND CORNU AMMONIS 2 AREA OF *PROECHIMYS*

C. A. SCORZA,[a] B. H. S. ARAUJO,[a] L. A. LEITE,[a] L. B. TORRES,[a,b] L. F. P. OTALORA,[c] M. S. OLIVEIRA,[d] E. R. GARRIDO-SANABRIA[c] AND E. A. CAVALHEIRO[a]*

[a]*Disciplina de Neurologia Experimental, Universidade Federal de São Paulo/Escola Paulista de Medicina, Rua Botucatu 862, 04023-900 São Paulo, Brazil*

[b]*Instituto Evandro Chagas, Centro Nacional de Primatas, Belém, Brazil*

[c]*Department of Biological Sciences, University of Texas at Brownsville and Center for Biomedical Studies, Brownsville, TX 78520, USA*

[d]*Departamento de Fisiologia e Farmacologia, Centro de Ciências da Saúde, Universidade Federal de Santa Maria, Rio Grande do Sul, Brazil*

Abstract—*Proechimys* (Rodentia: Echimyidae) is a neotropical rodent of the Amazon region that has been successfully colonized in the laboratory and used for experimental medicine. Preliminary studies indicated that *Proechimys* (casiragua) rodents express an atypical resistance to developing a chronic epileptic condition in common models of temporal lobe epilepsy. Moreover, previous investigation of our laboratory described a remarkably different Proechimy's cytoarchitecture organization of the hippocampal CA2 subfield. In the present study, we investigated the intrinsic neuronal properties and morphological characteristics of the *Proechimys*'s hippocampal pyramidal neurons of the CA1 and CA2 areas. A comparative approach was performed using neurons recorded in Wistar rats. A striking finding in *Proechimys* rodents was the presence of large pyramidal-like neurons throughout the stratum oriens from CA2 to CA1 area. In order to confirm such distinctive feature of the *Proechimys*'s hippocampus, we performed Nissl staining and immunohistochemistry for neurofilament protein SM311. CA2 pyramidal neurons in the stratum pyramidale of *Proechimys* exhibited a significantly higher input resistance and lower time constant when compared to corresponding cell groups in the same area of the Wistar rat's. This newly identified population of pyramidal-shaped neurons in stratum oriens of *Proechimys* exhibited distinct electrophysiological and morphological properties. This included larger capacitance, lower input resistance, larger rheobase, long latency to first action potential and slower firing frequency. In addition, the apical dendrites of these neurons were oriented in parallel to apical dendrites of regular pyramidal neurons in stratum pyramidale. Moreover, these neurons were immunoreactive to SM311 as the majority of the neurons of the pyramidal layer. The functional role of these hippocampal neurons of the rodent *Proechimys* deserves further investigation. © 2011 IBRO. Published by Elsevier Ltd. Open access under the Elsevier OA license.

*Corresponding author. Tel: +55-11-5573-9304.
E-mail address: esper@cgee.org.br (E. A. Cavalheiro).

Abbreviations: CA2, cornu ammonis 2; DIC, difference interference contrast; EPSCs, excitatory post-synaptic currents; EPSPs, excitatory postsynaptic potentials; HSD, honest significant difference; PBS, phosphate-buffered saline.

0306-4522/11© 2011 IBRO. Published by Elsevier Ltd. Open access under the Elsevier OA license.
doi:10.1016/j.neuroscience.2010.12.054

Key words: *Proechimys*, neurobiotin, hippocampus, stratum oriens.

Proechimys (Rodentia: Echimyidae) is a tropical rodent native to the Amazon region that has been successfully colonized in the laboratory and used for experimental medicine since 1964 (Hawking et al., 1964). Although originally utilized as hosts for infectious diseases research, these animals have recently attracted the attention of neuroscience research. *Proechimys* exhibit distinctive characteristics. For instance, immediately after offspring are born (usually one or two) they are capable of initiating locomotive activity and, to some degree, exploring their local environment. This indicates a higher degree of prenatal maturation of the nervous system when compared to other species of laboratory rats (i.e. Wistar and Sprague–Dawley).

Proechimys rodents live in complex environments in their natural habitats. Moreover, living in the wildness of rainforests may have put considerable selection pressures on these animals, especially on their nervous system, to adapt and survive predators. Certainly, their natural habitats offered more complex cues to their sensory system than any "artificial" environment can provide in the traditional vivarium conditions of experimental rats (i.e. Wistar, Sprague–Dawley). Compelling data indicate that domestication modifies (reduce brain's size) in several species (Ebinger, 1975; Kruska, 1975a,b; Kruska and Schott, 1977; Rohrs and Ebinger, 1999; Rehkamper et al., 2003; Kruska, 2005; Stuermer and Wetzel, 2006). For instance, several brain areas are smaller in laboratory rats versus wild Norway rats (Kruska, 1975a,b; Kruska and Schott, 1977). In this regard, *Proechimys* also offers a unique opportunity to investigate the anatomy and physiology of rodent nervous system structures, such as the hippocampus's involvement in cognitive mapping, sensory coding, memory, and so forth at different stages of evolution.

Previous study of our laboratory described a remarkably different Proechimy's cytoarchitecture organization of the hippocampal Cornu ammonis 2 (CA2) subfield (Scorza et al., 2010). We identified a very distinctive Proechimy's CA2 sector exhibiting disorganized cell presentation of the pyramidal layer and atypical dispersion of the pyramidal-like cells to the stratum oriens, strongly contrasting to the densely packed CA2 cells in the Wistar rats. Furthermore, *Proechimys*'s CA2 subfield presented significant higher density of calcium-binding proteins when compared to Wistar rats (Scorza et al., 2010). In addition, previous investigations of our group showed that *Proechimys* ro-

dents expressed an atypical resistance to developing a chronic epileptic condition in common models of temporal lobe epilepsy (Arida et al., 2005). In this line of evidence, *Proechimys* has been proposed as an animal model of resistance to epilepsy. Fabene at al. (2001) showed that the number of parvalbumin- or nitric oxide synthase-containing interneurons and their staining intensity were significantly increased in animals 30 days after status epilepticus. In addition, the number of glutamic acid decarboxylase (67)-immunoreactive interneurons was found to be markedly increased in the hilus and decreased in the CA1 pyramidal layer (Fabene et al., 2001). In general, due to *Proechimys*'s hippocampal intriguing characteristics, these rodents represent an extraordinary tool for neuroscience research.

The electrophysiological properties and individual morphological characteristics of principal neurons in the *Proechimys* hippocampus have yet to be explored. This information is critical to a better understanding of the *Proechimys* hippocampal network under normal conditions. Intrinsic neuronal properties are the electrophysiological signature of neurons critical for the functioning and operation of neuronal circuits. Therefore, it is critical to determine if these properties are different in Wistar versus *Proechimys* animals. In order to study these properties, we performed patch-clamp recordings from visually identified neurons in the hippocampus. These properties can be subdivided into passive neuronal properties, properties of the action potential (active), properties of afterpotentials—including afterdepolarizing potential (ADP) and afterhyperpolarizing potentials (AHP), firing phenotype (i.e. regular firing, fast spiking, and burst firing), firing frequency and accommodation.

During the development of the experiments, we noticed, by chance, that pyramidal-like cells appeared in the stratum oriens in brain slices of *Proechimys* rodents. The majority of the cells in the stratum oriens of Wistar rats are GABAergic interneurons and do not exhibit a pyramidal cell morphological phenotype. Therefore, we were highly intrigued by this observation. In this line of evidence, we decided to investigate these cells by performing electrophysiological (patch-clamp) recordings and by injecting the morphological tracer neurobiotin. In addition, we performed Cresyl Violet staining and immunohistochemistry (SMI311). SMI311 is a neuronal filament marker that preferentially labels neurons with pyramidal cell phenotypes in the hippocampus and cortex (Shetty and Turner, 1995; Sanabria et al., 2002). Electrophysiological experiments

Table 1. Intrinsic properties of pyramidal cells recorded in CA1 and CA2 area of hippocampus in Wistar rats versus *Proechimys*

Area Stratum	Wistar		*Proechimys*			ANOVA	
	CA1 Pyramidale *n*=8	CA2 Pyramidale *n*=7	CA1 Pyramidale *n*=7	CA2 Pyramidale *n*=11	CA1 and CA2 Oriens *n*=15	*F*	*P*-level
Passive membrane properties							
Capacitance, pF	60.2±28.3	51.6±23.8	36.6±14.1	45.5±16.2	151.4±56.2	12.81	0.0001
Resting membrane potential, mV	−61.8±3.7	−61.9±1.7	−65.1±3.1	−65.0±2.7	−62.0±2.5	1.75	0.15
Input resistance, MΩ	265.9±45.5	258.7±58.2	262.4±49.4	383.2±95.1	134.7±31.6	8.35	0.00005
Membrane time constant, ms	21.5±4.5	27.0±12.1	16.5±6.1	15.6±4.7	13.5±7.3	2.61	0.04
Active membrane properties							
Action Potential (AP) properties amplitude of AP, mV	113.0±11.2	100.1±11.3	104.3±11.2	103.3±10.8	107.7±11.1	1.05	0.41
AP threshold, mV	−46.1±2.3	−48.1±6	−50.7±5.3	−50.8±4.7	−49.0±4	0.92	0.46
Rheobase, pA	23.8±11.2	15.7±6.1	18.6±2.2	19.1±6.6	38.7±13.1	5.84	0.0007
AP half-height width, ms	2.2±0.4	2.2±0.3	2.6±0.2	2.7±0.4	2.2±0.2	1.98	0.09
Peak AP rise slope, mV/ms	141.3±24.5	108.5±15.5	101.6±29.1	104.2±33.2	127.7±30.3	1.50	0.21
Peak AP decay slope, mV/ms	−47.1±6.9	−44.2±4.4	−41.7±5.6	−37.9±9.3	−47.7±8.1	1.91	0.12
First AP latency, ms	53.8±5.5	47.1±4.5	60.0±10.5	120.9±20.9	232.7±90.5	5.5	0.001
Afterpotentials							
Afterdepolarization potential, mV	8.8±1.2	8.9±2.5	8.9±5.3	2.4±1.8*	6.8±1.5	5.53	0.001
Fast AHP, mV	−1.8±0.8	−1.9±0.6	−1.6±0.7	−2.3±1.1	−2.1±1.1	1.4	0.24
Medium AHP, mV	−2.1±0.5	−1.9±0.4	−3.0±0.9	−2.7±1.3	−1.7±0.7	0.21	0.92
Slow AHP, mV	−1.0±0.3	−0.8±0.25	−0.7±0.4	−0.7±0.4	−0.8±0.4	1.77	0.15
Firing frequency properties							
Interspike interval 1st spike, ms	37.9±5.5	21.9±4.6	33.1±5.6	32.8±8.8	51.0±15.5	0.45	0.76
Interspike interval last spike, ms	77.5±6.9	82.0±10.5	82.3±12.2	68.9±22.5	105.5±40.5	3.62	0.01
Maximal firing frequency, Hz	26.4±3.9	45.8±15.5	30.2±8.5	30.5±12.8	19.6±6.8	1.7	0.06
Steady-state frequency, Hz	12.9±4.3	12.2±4.2	12.9±5.6	14.5±6.3	9.5±4.5	4.5	0.04
Adaptation index	0.5±0.08	0.3±0.09	0.4±0.05	0.5±0.1	0.5±0.12	1.48	0.22
Depolarizing "sag"							
Sag ratio	0.93±0.2	0.95±0.2	0.91±0.2	0.91±0.1	0.97±0.3	4.18	0.01
Sag amplitude, mV	4.9±1.4	3.7±2.5	10.3±3.1	10.0±3.8	2.8±1.1	3.1	0.02

Data presented as mean±standard deviation. AHP, afterhyperpolarization.

* Only two out of 11 cells presented active afterdepolarization (ADP).

were also performed to investigate the intrinsic membrane properties of the newly identified pyramidal cell-like neurons in stratum oriens and the synaptic connectivity of these neurons as well.

EXPERIMENTAL PROCEDURES

Animals

Twenty-nine male *Proechimys* animals (7–45 days old) and 11 male Wistar rats (7–45 days) were used in these experiments. *Proechimys* rodents, originally from the Brazilian Amazon basin, were bred in a colony established at the Universidade Federal de São Paulo/Escola Paulista de Medicina and housed in a standard light–dark cycle with free access to food and water. Wistar rats of the same age and sex were obtained from the laboratory colony. The procedures involving the animals and their care at the Experimental Neurology Laboratory of the Federal University of São Paulo respected the Institution's guidelines, which comply with national and international rules and policies.

Hippocampal slices and patch-clamp recordings

To accomplish this objective, we developed patch-clamp recordings from visually identified pyramidal cells in the hippocampal slices taken from Wistar and *Proechimys* rats (7–30 days). Horizontal slices were prepared with a Campden Vibratome using a dissecting media composed of (in mM): 251 sucrose, 3 KCl, 2 $CaCl_2$, 2 $MgSO_4$, 2 $MgCl_2$, 1.25 NaH_2PO_4, 21 $NaHCO_3$, and 10 glucose, aerated with 95% O_2–5% CO_2 (pH 7.4; 300–310 mOsm). Individual slices were then transferred to a recording chamber positioned in the stage of upright Nikon's E600FN physiology microscope that was continuously perfused with artificial cerebrospinal fluid (ACSF) with the following composition (in mM): normal ACSF=129 NaCl, 3 KCl, 1.6 $CaCl_2$, 2 $MgSO_4$, 1.25 NaH_2PO_4, 21 $NaHCO_3$, and 10 glucose, aerated with 95% O_2–5% CO_2 (pH 7.4; 300–303 mOsm). Whole-cell patch clamp recordings were made

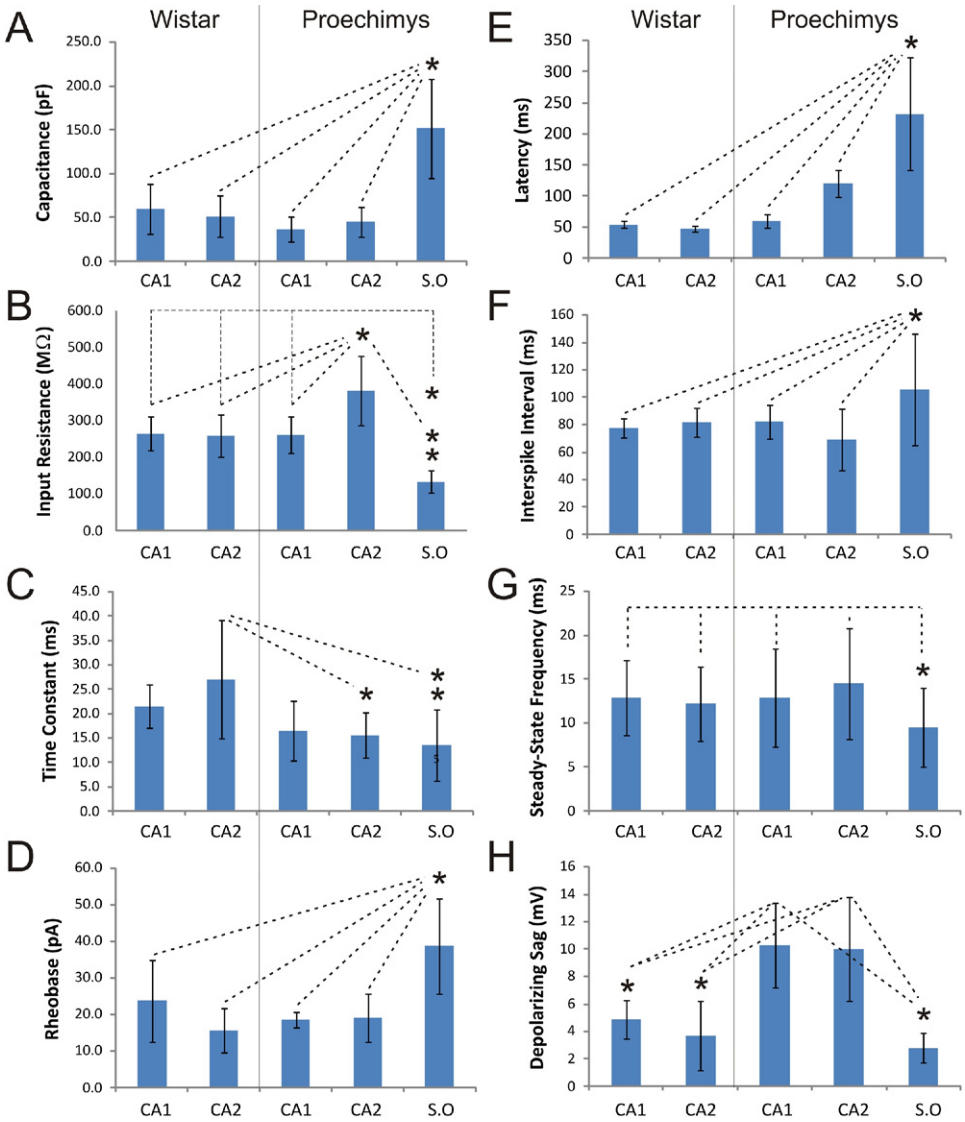

Fig. 1. (A–H) Graph representing differences in intrinsic membrane properties and representation of statistical analysis using post-hoc Tukey's HSD test in data sets that were significantly different by one-way ANOVA. * $P<0.01$, ** $P<0.001$. For interpretation of the references to color in this figure legend, the reader is referred to the Web version of this article.

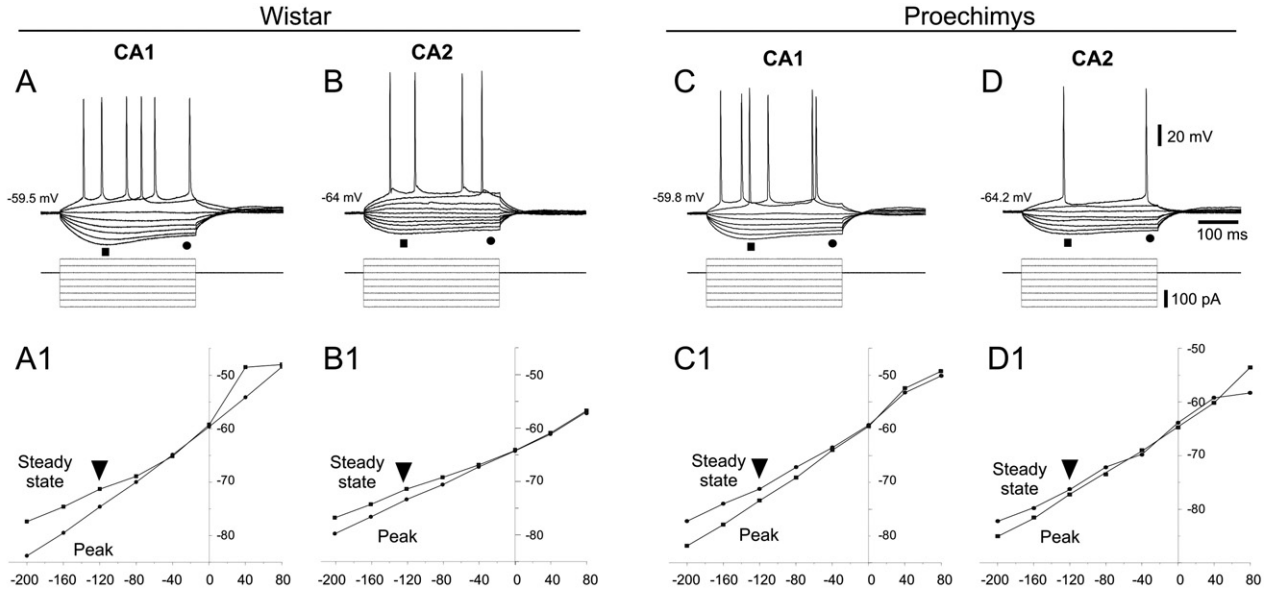

Fig. 2. The depolarizing sag in Wistar and *Proechimys* pyramidal layer neurons in response to intracellular application of hyperpolarizing current pulses. (A–D) Representative examples of responses of recorded neurons to different intensities of hyperpolarizing current pulses in CA1 and CA2 areas of Wistar (A and B respectively) versus *Proechimys* animals (C and D respectively). Notice that CA1 neurons exhibited stronger inward rectification (higher depolarizing "sag") than CA2 neurons. Current injection protocols are depicted below voltage traces. (A1–D1) Voltage-current relationships of these neurons measured at the negative peak (■) and at the steady state (●) of the voltage deflection. Notice inward rectification at more hyperpolarized potentials more negatives than −80 pA (see arrowheads in steady-state curves, A1–C1). Inward rectification was not very evident in *Proechimys* CA2 pyramidal layer neurons (D1).

from visually identified pyramidal neurons in the CA1 and CA2 regions of the hippocampus. The transition from CA2 to CA1 was defined by inspection of the hippocampus at low magnification using difference interference contrast (DIC) imaging (×4) prior recordings. In both species pyramidal layer appeared wider in CA2 area. After switching to ×40 objectives, neurons were initially

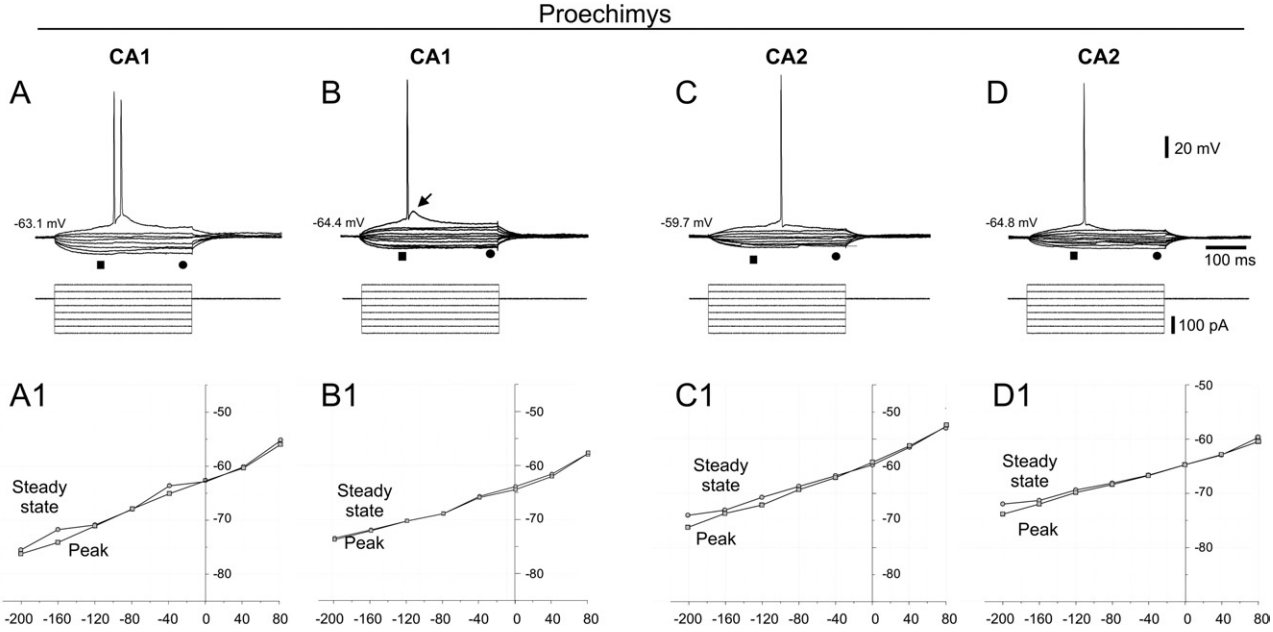

Fig. 3. Pyramidal-like neurons recorded in CA1 and CA2 areas of stratum oriens in *Proechimys* exhibited minimal to no hyperpolarization-activated depolarizing sag in current clamp mode of whole patch-clamp configuration. (A–D) Representative examples of voltage traces triggered by current injection protocols (depicted below) in different cells recorded in CA1 (A, B) and CA2 (C, D) subfields. Notice that these neurons also exhibited small input resistance and long latency to generate first action potential. Burst (2 spike) firing was observed in a CA1 neuron (A) while the other neuron expressed a pronounced ADP (arrow in B). Notice that input membrane resistance is higher in CA1 versus CA2 neurons. (A1–D1) Voltage-current relationships of these neurons measured at the negative peak (■) and at the steady state (●) of the voltage deflection showing an almost linear relationship with minimal inward rectification at the steady state.

identified on the basis of soma shapes using infrared illumination and DIC optics (IR-DIC). Recordings were performed in stratum radiatum and stratum oriens. Recording pipettes pulled from borosilicate glass had a resistance of 5–7 M. Patch clamp electrodes were filled with a solution comprising (in mM): 120 K-gluconate, 10 KCl, 1 $MgCl_2$, 2.5 Mg-ATP, 10 HEPES, 0.25 Na_2-GTP, 0.1 BAPTA, and Neurobiotin 0.1% (pH 7.2; 287 mOsm). Intrinsic membrane properties were recorded in current-clamp mode using an AXOPATCH-1D amplifier. Excitatory post-synaptic currents (EPSCs) were recorded using voltage-clamp configuration. Pyramidal neurons were voltage clamped at −70 mV. Series and access resistance were monitored continuously, and cells were discarded if access resistance changed by >25%. Data were digitized at 10 kHz with a DIGIDATA 1300 A/D board (Axon Instruments, Foster City, CA, USA) and stored on a PC running pClamp8 software (Axon Instruments).

Schaffer collateral fiber stimulation

To evoke orthodromic ("synaptic") responses, brief (100 μs) stimuli were delivered using Teflon-coated tungsten bipolar electrodes (10–20-μm tips) positioned in the Schaffer collateral region in the stratum radiatum near CA2. Electrical voltage pulses (100–150 μs) were delivered through a constant-current isolation unit (DS2, Digitimer, Hertfordshire, UK). Excitatory postsynaptic potentials (EPSPs, current clamp) and EPSC (voltage-clamp) were spontaneously recorded or evoked by Schaffer collateral electrical stimulations at a frequency of 0.05–0.033 Hz. Stimulus strengths were adjusted to evoke reproducible response amplitudes (70% of the maximal amplitude). Stimulation intensities ranged from 0.2 to 10 mV. Paired pulse protocols (50-ms or 100-ms interpulse interval) were used to study short-term plasticity. Analysis of intrinsic properties was performed off-line using the software Clampfit 9

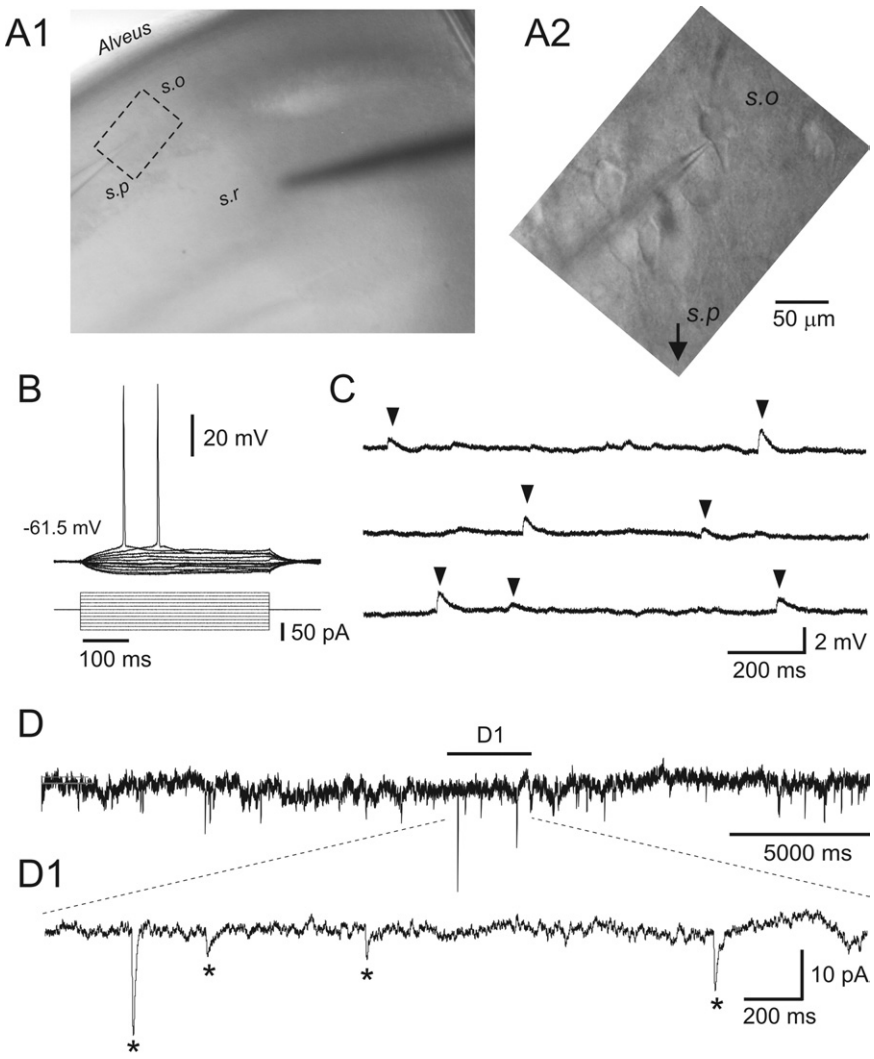

Fig. 4. Pyramidal-like neurons in stratum oriens of *Proechimys* receive spontaneous excitatory synaptic activity. (A1) Representative hippocampal slice at low magnification (×5) indicating the positioning of recording electrodes in stratum radiatum. (A2) Pyramidal-like neurons positioned in stratum oriens were visualized using infrared (IR)-difference interference contrast (DIC) optics at high magnification (×40). Notice several neurons with a pyramidal-shaped soma and apical dendrites running in parallel towards the pyramidal layer. One of these neurons was recorded using a patch-clamp pipette to monitor intrinsic neuronal properties and synaptic connectivity. (B) Voltage traces in response to current injection (below) in current-clamp recorded neuron depicted in (A1). Observe low input resistance and slow firing frequency. (C) Spontaneous excitatory postsynaptic potentials of different amplitudes (arrowheads) impinging on the recorded neuron. (D) After switching to voltage clamp (holding potential=−70 mV), intense spontaneous synaptic activity in the form of excitatory postsynaptic currents (EPSCs) were detected on the cell. (D1) Expanded time scale of a segment from current trace in (D) to visualize with better resolution the different EPSCs (*).

(Molecular Devices, CA, USA) and presented in table and graphs. Statistical analysis was performed using one-way ANOVA and post-hoc comparison tests and using Student's *t*-test. Significance was set at $P<0.05$.

Morphological identification of recorded neurons

At the end of the recordings, slices were removed from the recording chamber and fixed overnight in 4% paraformaldehyde and 15% picric acid in 0.1 M phosphate buffer (PB), pH 7.4. The slices were then washed several times in 0.01 M phosphate-buffered saline (PBS) before incubation with 0.5% H_2O_2 in 0.1 M PBS for 90 min to reduce endogenous peroxidase activity and background staining. After washing, nonspecific binding was prevented by incubating the sections for 1 h with 5% normal goat serum (NGS, DAKO, Denmark) in 0.1 M PBS and 0.3% Triton X-100. Subsequently, slices were incubated with avidin-biotin peroxidase (diluted 1: 100; ABC, Vector Laboratories) in 1% NGS (DAKO, Denmark) and 0.3% Triton X-100 overnight at 4 °C. Slices were then washed in 0.1 Triton X. Injected neurons were visualized using avidin-biotinylated horseradish peroxidase complex reaction (ABC; Vector Laboratories, Burlingame, CA, USA) with 3,3-diaminobenzidine (DAB) (Sigma, St. Louis, MO, USA) as chromogen (brown reaction product). After dehydration and embedding in mounting media, the representative neurons were reconstructed using NeuroLucida software (MicroBrightField, Inc., Colchester, VT, USA). Labeled pyramidal neurons exhibiting a relatively large number of neurobiotin-filled dendritic were reconstructed, and morphological parameters were quantified in combination with an automated stage and focus control connected to the microscope (Carl Zeiss, Germany). Data were collected as line drawings, consisting of X, Y, and Z coordinates. Numerical analysis and graphical processing of the neurons were performed with NeuroExplorer (MicroBrightField). Statistical analysis was performed using one-way

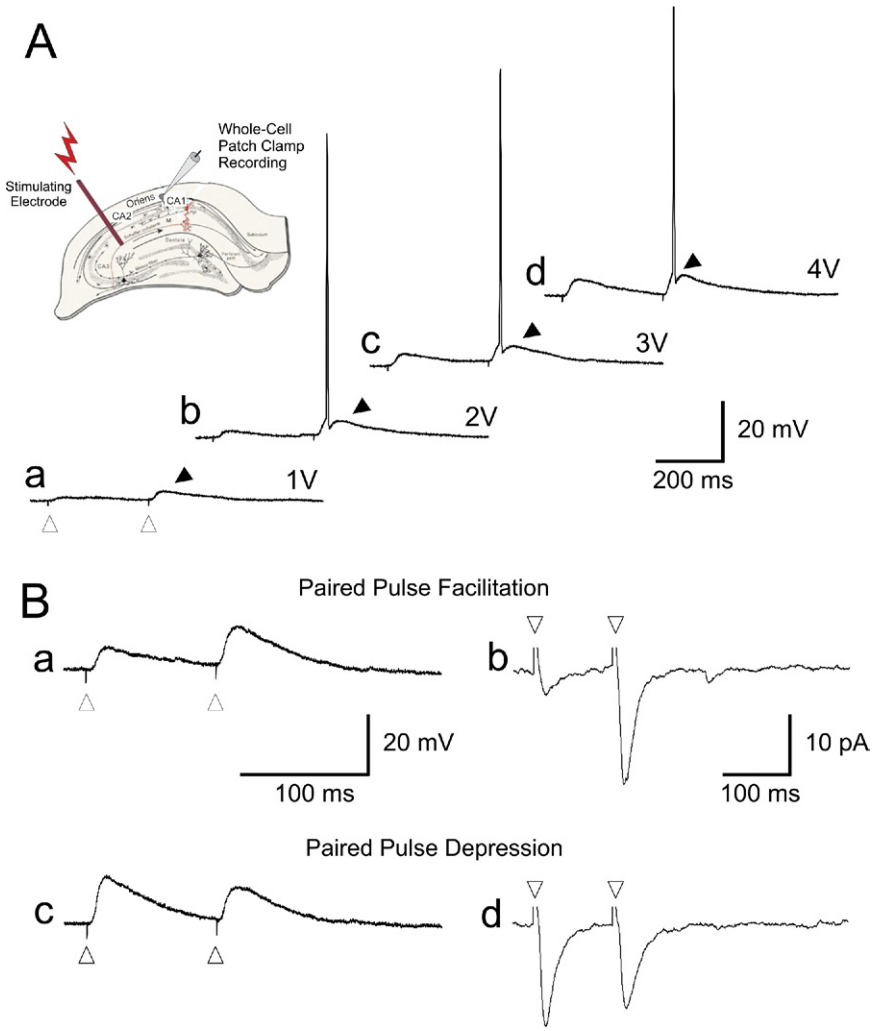

Fig. 5. Pyramidal-like neurons in stratum oriens of *Proechimys*'s hippocampus receive excitatory inputs via Schaffer collaterals. (A) Paired-pulse stimulation of Schaffer collateral pathway triggered a first synaptic response (EPSP). A second EPSP of larger amplitude (paired-pulse facilitation, black arrowheads), eliciting in some cases an action potential stimulation intensity, is shown at the end of each voltage trace (a–d). (Inset: Schematic representation of the recording and stimulation configuration for these experiments, white arrowheads represents stimulation artifacts). (B) Stimulation paradigms evoked paired pulse facilitation of EPSPs (a) in current-clamp and EPSCs in voltage clamp (c, holding potential −70 mV) at stimulation intensity of 2 V. At higher stimulation intensity (5V), a similar paradigm evoked paired-pulse depressions of the second synaptic response (EPSP in "b" or EPSC in "d"). Stimulation artifacts represented by white arrowheads. For interpretation of the references to color in this figure legend, the reader is referred to the Web version of this article.

ANOVA and Turkey post-hoc tests. Significance was set at $P<0.05$.

Tissue preparation, Cresyl Violet staining and immunohistochemistry

A set of three adult male Wistar and three juvenile male *Proechimys* rats (45–60 days old) were used for the study. Anaesthetized animals were perfused transcardially with 0.1 M PBS followed by 4% paraformaldehyde in PBS. The brains were removed immediately after perfusion, post-fixed in the same fixative solution for 4 h. Brains were sectioned in 40 μm thickness, using a vibratome, collected, and washed with PBS (pH 7.4). Paired sections from Wistar and *Proechimys* rats at matched anteroposterior levels were processed in the same vial in order to minimize the intergroup differences during the immunohistochemical procedure.

Several sections were Nissl-stained (Cresyl Violet) to assess cytoarchitectonic boundaries and the characteristics of hippocampal subfields. In addition, Nissl staining was used to detect whether pyramidal-like cells appear in the stratum oriens. Corresponding free-floating sections were selected from both Wistar and *Proechimys* rat groups and processed simultaneously. All sections were treated with 0.1% H_2O_2 in PBS to quench endogenous peroxidase and then incubated for 30 min in PBS containing 0.3% Triton X-100. After that, the sections were incubated for 2 h in 5% bovine serum albumin in PBS and then once again incubated overnight with the primary antibody. For studying the pyramidal-cell like neurons in stratum oriens, we used (1:1000 Anti-Pan-Neuronal Neurofilament Marker SMI311, monoclonal mouse mAb, Calbiochem, USA) in the presence of 1% bovine serum albumin. In addition, we performed dual fluorescence immunostaining using guinea pig polyclonal antibody anti-vesicular glutamate transporter type 1 (VGluT1) (1:5000, Millipore, USA). VGluT1 is expressed in glutamatergic terminals. After incubation in primary antibody, sections were washed three times in PBS. Then, the sections were incubated with the secondary antibody (i.e. conjugated to biotin or to Alexa Fluor fluorescent dye 488 and 568, 1:200, Invitrogen). For biotinylated secondary antibodies, immunodetection was performed using the Vectastain ABC Elite Kit (Vector Burlingame, CA, USA) and the complex antigen–antibody was visualized using diaminobenzidine in TBS and H_2O_2 (1 μl/ml). Tissue sections were mounted on glass slides and coverslipped with either regular mounting media or fluorescent safe mounting media.

The material processed with DAB and the sections stained with Cresyl Violet were studied with a microscope using bright-field illumination. Results were visualized, and pictures were acquired using a Zeiss Axioskop 2 microscope, AxioCam HR CCD 24-bit camera and AxioVision software (Zeiss, Oberkochen, Germany). Data from immunofluorescence were analyzed using Olympus Fluoview Confocal Microscopy. Fluorescent signals were captured by using a computerized acquisition system Fluoview FV300 and an inverted confocal laser scanning microscope (Leeds Precision Instrument Inc., MN, USA) equipped with argon (488 nm) and krypton (568 nm) lasers for Alexa Fluor 488 (emission by 505–550 nm bandpass filter) and Alexa Fluor 568 (emission by 585 nm long-pass filter) imaging, respectively. The two fluorophores were acquired separately and combined in Fluoview. For immunofluorescence quantification, several corresponding sectors (50 μm diameter) were selected for analysis in a mossy fiber termination zone (stratum lucidum) and in hilus of dentate gyrus. To allow direct comparison of different data sets, imaging was performed using the same parameters for laser excitation (i.e. intensity) and photomultiplier tube detection (i.e. sensitivity) in each set of samples.

RESULTS

Intrinsic properties of pyramidal neurons in CA1 and CA2 hippocampal areas of Wistar versus *Proechimys*

A total of 55 neurons were recorded in CA1 and CA2 areas of hippocampal slices taken from seven Wistar and 10 Proechimy animals. Six of these neurons (three in Wistar and three in *Proechimys*) exhibited a firing phenotype typical of GABAergic neurons (fast spiking). We focused our study on non-fast spiking neurons ($n=48$). From these neurons, 15 cells were recorded in the stratum pyramidale from six Wistar rats slices (CA1: $n=8$ and CA2: $n=7$, Table 1). Thirty-three cells were recorded in the stratum pyramidale ($n=19$, CA1: $n=8$ and CA2: $n=11$) and in the stratum oriens ($n=15$) of hippocampal slices taken from 10 *Proechimys* animals (Table 1). Neurons in the stratum oriens were selected for electrophysiological recordings if they exhibited distinctive pyramidal cell-like morphological features during IR-DIC visualization (i.e. triangular somata, approximately 8 μm cross-sectional diameter or more, apical dendrites oriented towards stratum pyramidale and in parallel to orientation of apical dendrites of pyramidal cells). Healthy pyramidal-like cells exhibited relatively large somas (10–25 μm diameter range) when compared to pyramidal cells in the stratum pyramidale. They were usually visualized deep in the slice across the stratum oriens,

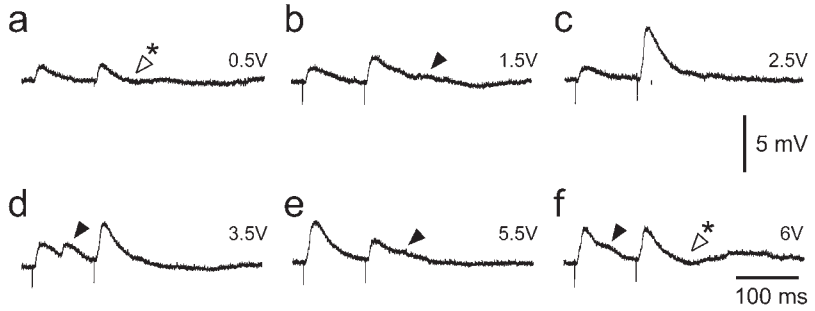

Fig. 6. Pyramidal-like neurons recorded in stratum oriens of *Proechimys* rats receive simple and complex synaptic afferents from Schaffer collateral pathway. Typical monoexponentially decaying EPSP were observed (first EPSP in "a, b, c" and second EPSP in "a" and "d") in pyramidal-like neurons recorded in stratum oriens. An EPSP-inhibitory postsynaptic potential (IPSP) sequence (* white arrowheads in "a" and "f") was evoked in these neurons by stimulation of the Schaffer collateral-commissural pathway in hippocampal slices. In some cases, more complex EPSP responses were observed (first EPSP in "d" and "f", see arrowhead and second EPSP in "b" and "e", arrowheads), indicating possible feedforward activation of an excitatory local circuit or activation of different synapses with different synaptic time delays.

were more abundant in the first 100 μm above the pyramidal layer and were selectively distributed in CA1 and CA2 subfields. We were unable to detect these neurons in the CA3 stratum oriens.

The statistical analysis of passive and active intrinsic properties revealed a significant difference by one-way ANOVA of the following variables: capacitance (Cm), input resistance (Rm), membrane time constant (τ), rheobase (Rh), latency to the first action potential, afterdepolarizing potential, interspike interval for the last spike in the 200–400 ms, steady-state frequency (>200 ms), and the depolarization "sag" ratio and amplitude, which is representative of the hyperpolarization-activated cationic current (I_h) (Table 1). In Wistar CA1 pyramidal cell layer, one out of eight cells fired a 2 spike burst while the remaining cells exhibited a regular firing phenotype. All the cells in the CA2 area showed regular firing characteristics in both species. All the cells in the pyramidal layer (CA1 and CA2 areas) of both species exhibited spike frequency adaptation (accommodation). In *Proechimys*, one out of 15 pyramidal-like cells in stratum oriens exhibited a 2 spike bursting phenotype while the remaining cells exhibited regular firing properties.

Statistical analysis of the capacitance show that *Proechimys* CA1 and CA2 pyramidal-like cells in the stratum oriens exhibited significantly higher capacitance (Table 1) when individually compared to all other groups by the post-hoc Tukey's HSD for honest significant difference test, $P<0.05$ (Fig. 1A, *). However, no differences were detected among CA1 and CA2 cells recorded in the pyra-

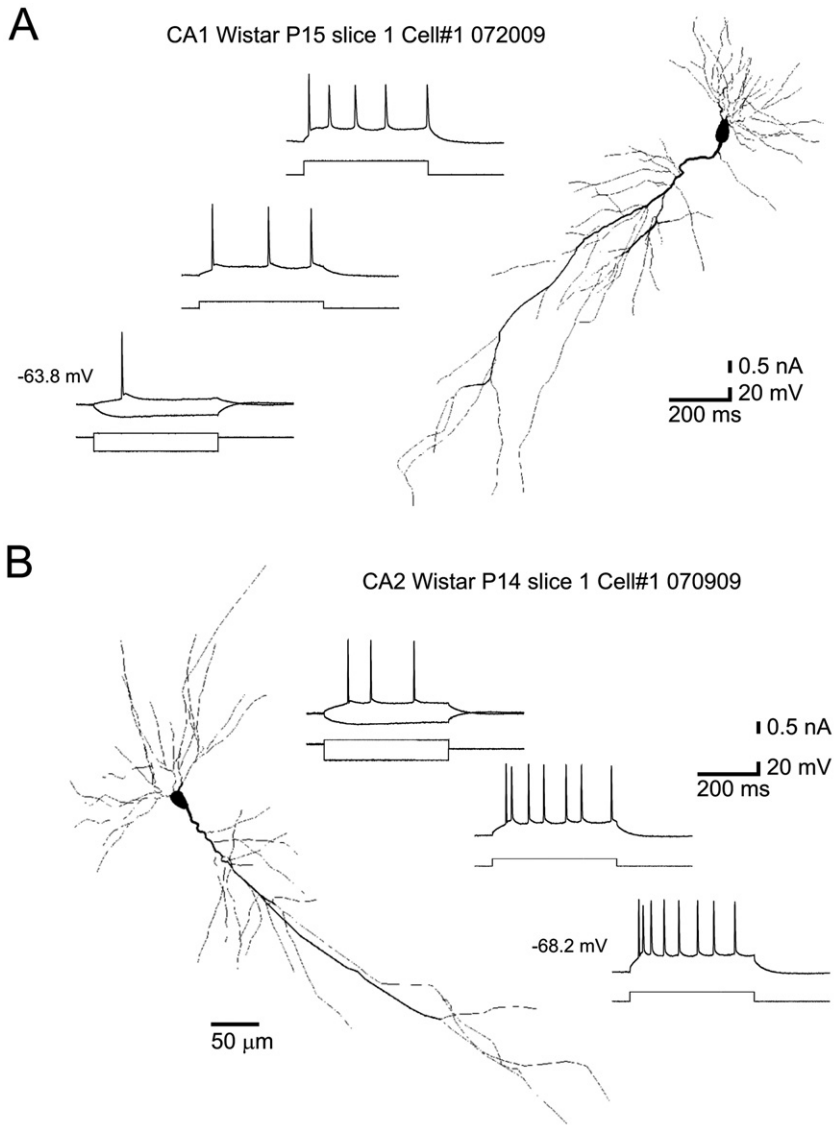

Fig. 7. Electrophysiologically characterized neurons in CA1 and CA2 area (pyramidal layer) of Wistar rat (A and B respectively) that were filled with neurobiotin to reveal morphological features. Notice typical pyramidal shape and distribution of apical and basal dendrites. Patch-clamp recordings in current clamp configuration revealed a regular firing pattern evoked by different steps of square depolarizing current pulses (represented below electrophysiological traces).

midal layer of Wistar and *Proechimys* hippocampal slices (Fig. 1A). Input resistance in CA2 pyramidal layer cells of *Proechimys* was significantly different than CA1 and CA2 cells (stratum pyramidale) of Wistar rats (Post-hoc Tukey's HSD test, $P<0.001$ respectively) and CA1 pyramidal layer cells of *Proechimys* (Post-hoc Tukey's HSD test, $P<0.001$). In addition, a significant difference was observed between CA2 pyramidal cell layer cells and stratum oriens pyramidal-like cells (CA1 and CA2) of *Proechimys* (Post-hoc Tukey's HSD test, $P<0.0001$). Pyramidal-like cells in stratum oriens were significantly different than all groups when compared by post-hoc analysis (Tukey's HSD test) (Fig. 1B). Furthermore, membrane time constants of CA2 cells in pyramidal layer of Wistar rats was significantly different than CA2 cells in the pyramidal layer of Wistar (Tukey's HSD test, $P<0.01$) and pooled CA1 and CA2 cells with a pyramidal phenotype in stratum oriens of *Proechimys* (Tukey's HSD test, $P<0.001$) (Fig. 1C). The amount of current necessary to evoke an action potential at the resting membrane potential (rheobase) in pyramidal neurons of *Proechimys*'s stratum oriens was significantly higher ($P<0.01$ Tukey's HSD test) when compared to each of the experimental groups (Fig. 1D, Table 1). In similar fashion, the latency to the first action potential at threshold and the interspike interval in the last spike of 400-ms injection current protocol were significantly longer in these pyramidal cells when compared to pyramidal layer neurons in both Wistar and *Proechimys* (Fig. 1E, F, Table 1). These pyramidal-like neurons also exhibited slower steady-state frequency (Fig. 1G, Table 1).

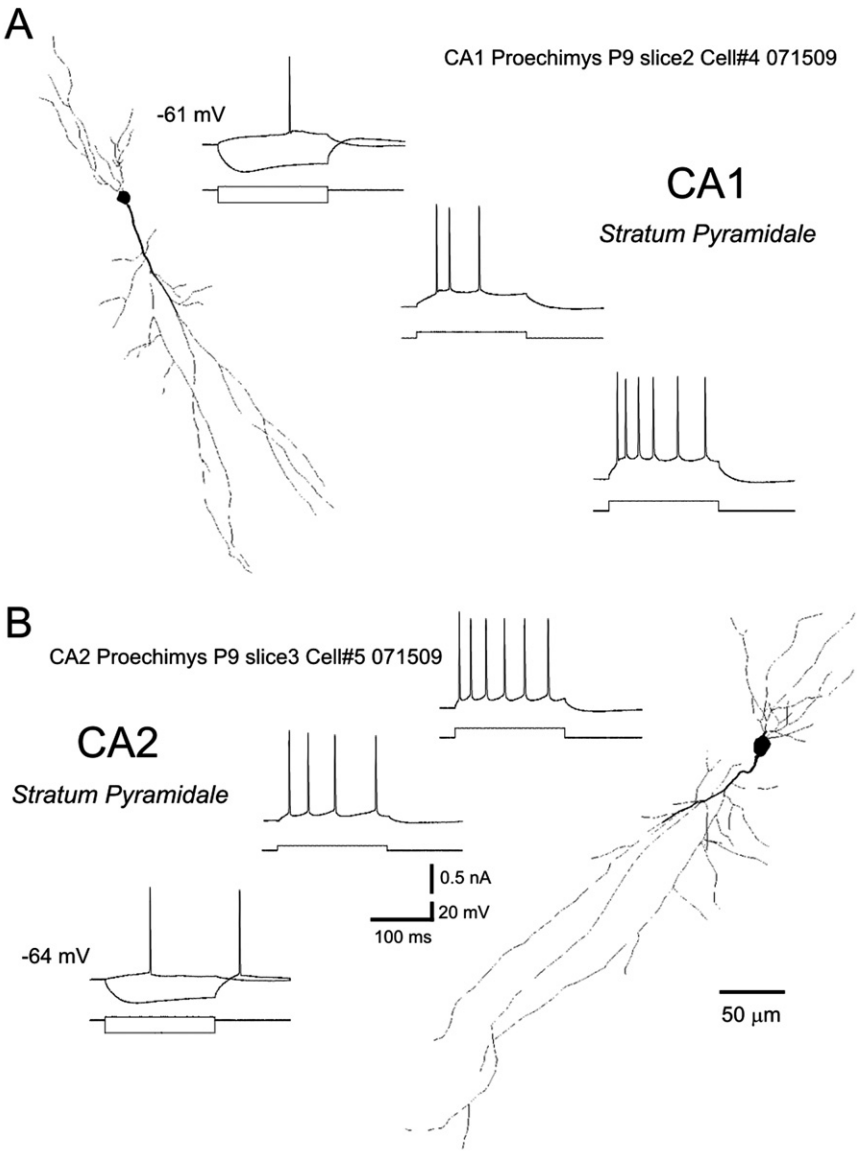

Fig. 8. (A, B) Electrophysiologically characterized neurons in CA1 and CA2 areas (pyramidal layer) of *Proechimys* that were filled with neurobiotin to reveal morphological features. Electrophysiological recordings in current clamp revealed a regular firing phenotype evoked by depolarizing current steps (insets) and pronounced depolarization sags when hyperpolarizing currents were injected indicative of a large hyperpolarization-activated current I_h in these cells.

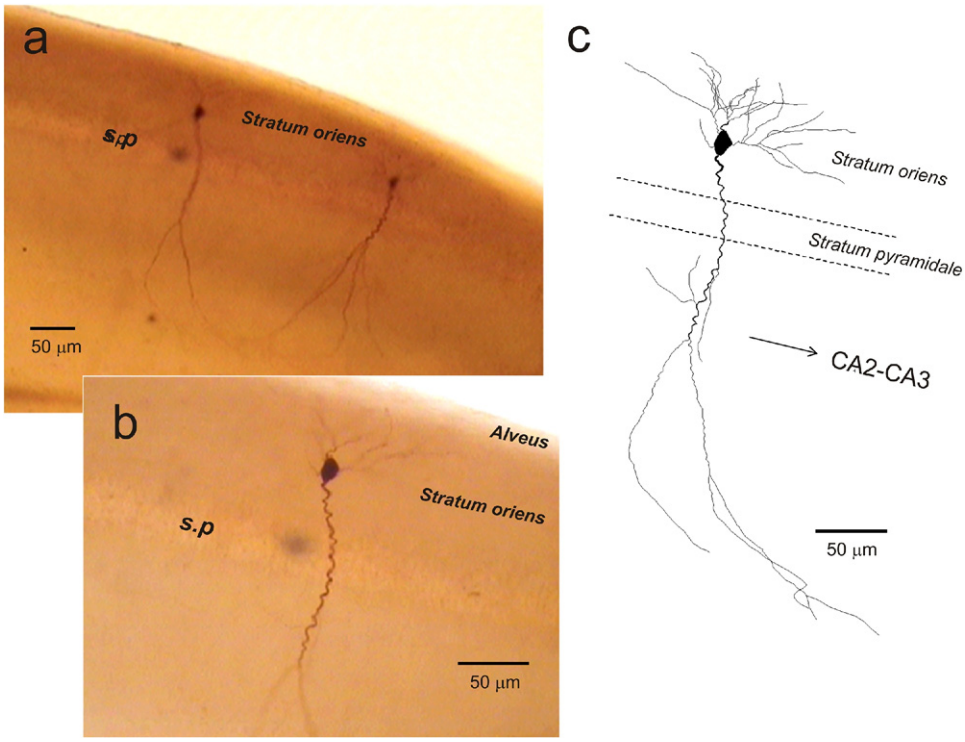

Fig. 9. Pyramidal-like neurons in stratum oriens of CA1 subfield in *Proechimys*. (a) Image of slice containing two neurobiotin-filled neurons recorded in stratum oriens (s.o.) of *Proechimys*. (b) Higher magnification of left neuron that was reconstructed using Neurolucida Stereoinvestigator software. Notice position of the cells in the middle of s.o. For interpretation of the references to color in this figure legend, the reader is referred to the Web version of this article.

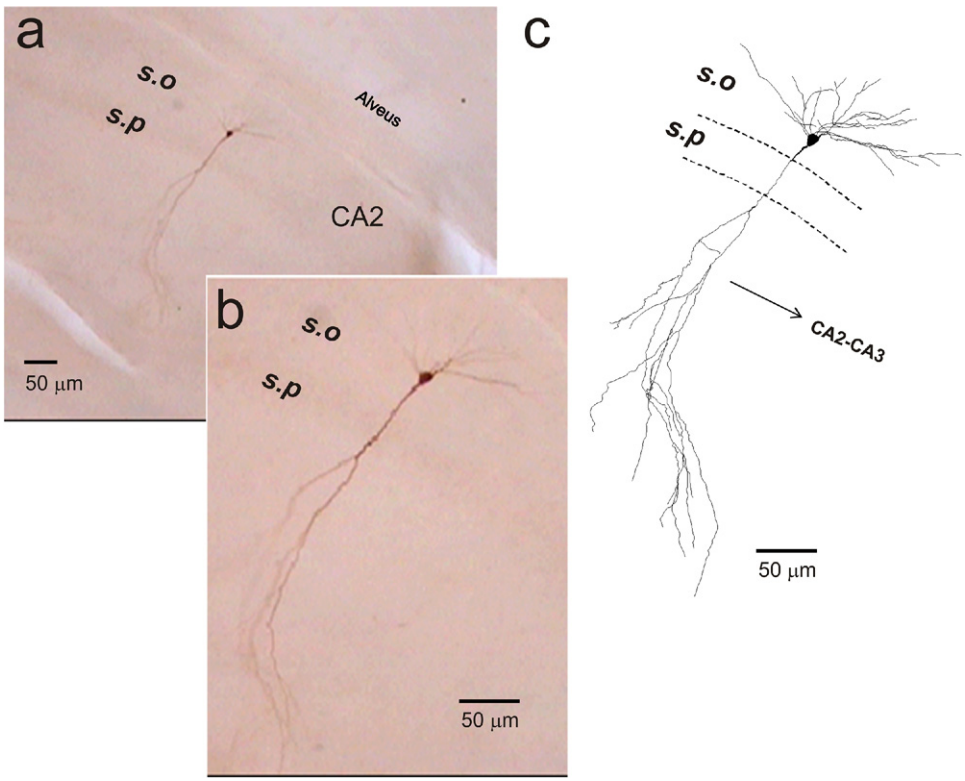

Fig. 10. Pyramidal-like neurons in CA1 area of stratum oriens of *Proechimys*. (a) Image of slice one neurobiotin-filled neurons recorded in stratum oriens (s.o.) of *Proechimys*. (b) Higher magnification of neuron that was reconstructed using Neurolucida Stereoinvestigator (c). For interpretation of the references to color in this figure legend, the reader is referred to the Web version of this article.

Hyperpolarizing current pulses revealed a depolarizing sag in the vast majority of the neurons in CA1 and CA2 pyramidal layer of both Wistar and *Proechimys*. The depolarizing sag disappeared at voltages close to the baseline membrane potential (see the plot in Fig. 2A1–D1) and was constantly activated at hyperpolarized levels. In approximately 60% of CA1 neurons in Wistar and *Proechimys* animals, the offset of current pulse produced a rebound depolarization and firing while this effect was only observed in 10% of CA2 pyramidal layer neurons. Statistical analysis revealed that neurons in the CA1 and CA2 pyramidal layer of *Proechimys* exhibited significantly higher depolarizing sag than both classes of neurons in Wistar rats (Table 1, Fig. 1H). However, pyramidal-like neurons recorded in the stratum oriens exhibited significantly smaller depolarizing sag (or was absent in some cases) when compared to CA1 and CA2 pyramidal layer neurons in *Proechimys* (post-hoc Tukey's HSD, $P<0.01$ for both comparisons, Figs. 1H and 3). No significance difference was detected when compared to CA1 and CA2 pyramidal layer cells in Wistar rats.

We also compared the intrinsic properties between pyramidal-like cells recorded in CA1 versus CA2 of the stratum oriens of *Proechimys*. The statistical analysis indicates that the input resistance was the only electrophysiological variable (passive membrane properties) that significantly varied between stratum oriens CA1 and CA2 pyramidal-like cells (164 ± 8.3 mΩ in CA1 cells $n=5$ vs. 120.1 ± 24.4 mΩ in CA2 cells $n=10$, a 29.1% reduction, Student t-test $P<0.01$). This difference is illustrated in Fig. 3. Notice that CA1 neurons (A, B) exhibit larger input resistance than CA2 cells (C, D). Since no significant changes were observed among all the other membrane properties (Student t-tests, $P>0.05$), CA1 and CA2 pyramidal-like cells in stratum oriens were then pooled together for statistical analysis.

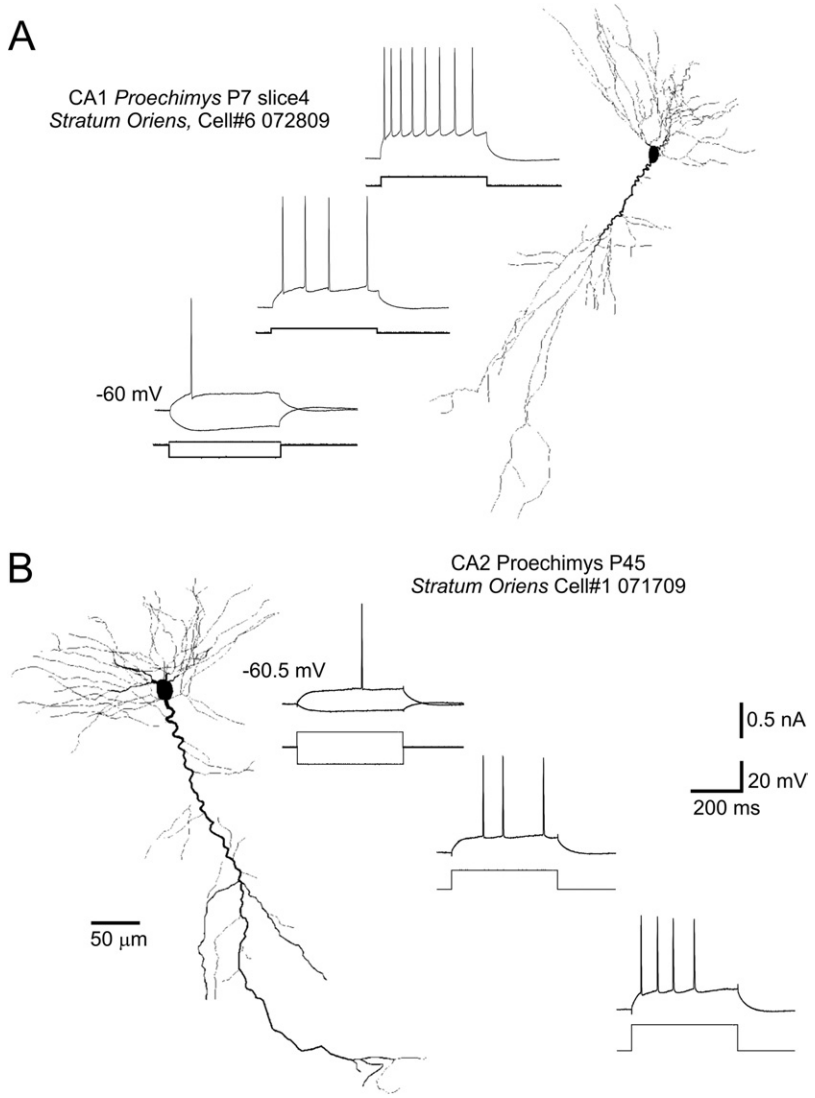

Fig. 11. Electrophysiological properties of pyramidal-like neurons in stratum oriens CA1 area (A) and CA2 area (B) of *Proechimys*. Notice the pyramidal shape of soma and typical apical and basal dendrites of pyramidal neurons. Electrophysiological recordings indicate that these neurons exhibited a regular firing repertoire upon injection of depolarizing current steps.

Pyramidal-like neurons receive synaptic inputs from other neurons and are integrated into hippocampal networks of *Proechimys*

After characterizing the intrinsic membrane properties of pyramidal-like cells in the stratum oriens of the hippocampus of *Proechimys* (Fig. 4A1, IR-DIC visualized slice with recording pipette and stimulating electrode at low magnification ×5), we investigated whether these pyramidal-like neurons (Fig. 4A2, notice pyramidal shapes and apical dendrites oriented towards pyramidal cell layer as visualized by IR-DIC at ×40 magnification during recording section) receive excitatory synaptic connections from neighboring neurons. To address this question, we first monitored the presence of spontaneous background EPSPs (current clamp) or EPSCs (voltage clamp) impinging on the recorded neurons. We detected that all 15 neurons recorded in this area received different levels of synaptic inputs including EPSPs (Fig. 4C) or EPSCs (Fig. 4D, D1, *). Spontaneous synaptic activity may emerge from different hippocampal or extrahippocampal pathways. To explore whether stratum oriens' pyramidal-like neurons receive input from intrahippocampal neurons, we positioned stimulating bipolar electrodes in the stratum radiatum in the anterior portion of the CA2 subfield to stimulate the Schaffer collateral pathway. The Schaffer collateral consists of axons originating from hippocampal CA3 pyramidal neurons that evoke a short latency excitatory (glutamatergic) synaptic response in CA1 and CA2 stratum pyramidale neurons (Davies and Collingridge, 1989).

Evoked synaptic responses were studied in six pyramidal-like neurons in stratum oriens by positioning a stimulating electrode in the stratum radiatum of the slices (Fig. 4A). Stimulation of the Schaffer's collateral pathway triggered synaptic responses in both current clamp (i.e. evoked EPSP) and voltage clamp configuration (EPSCs). In current-clamp configuration, paired pulse stimulation with 50- or 100 ms inter-stimulus interval evoked EPSPs with typical paired-pulse facilitation of the second response (Fig. 5Aa), which is typical of synapses from CA3 pyramidal cell upon CA1 pyramidal cell dendrites (i.e. low release probabilities) (Debanne et al., 1996; Stricker et al., 1996). An EPSP-inhibitory postsynaptic potential (IPSP) sequence was evoked in CA1 neurons by stimulation of the Schaffer collateral-commissural pathway in rat hippocampal slices as previously reported in Wistar CA1 pyramidal neurons (Davies and Collingridge, 1989). The increase in amplitude of the second EPSP was able to trigger action potentials (Fig. 5Ab–d). This indicates that these pyramidal-like neurons in stratum oriens receive afferents from Schaffer collateral pathway, and these cells relay information as part of the hippocampal network. At low stimulation intensity (<3 V), all the stimulated cells exhibited paired-pulse facilitation of evoked synaptic responses (Fig. 5Ba, c). At higher stimulation intensity (>4 V), five out six neurons exhibited paired-pulse depression (Fig. 5Bb, d).

In two out of the six neurons, we noticed that Schaffer collateral stimulation triggered not only single monoexponentially decaying EPSP (Fig. 6a, c) but also complex EPSP responses. These included multiple peaks (Fig. 6d, two peaks in the first response) or complex responses with a non-exponential decay (Fig. 6b, e, f). These responses may represent simultaneous activation of several inputs to the cell, a local feed forward excitatory input, or a fast recurrent excitatory connection into these pyramidal-like neurons. In general, our data indicate that these neurons in stratum oriens receive excitatory inputs from Schaffer collateral pathway that can originate in the CA3 pyramidal layer or in local CA1 pyramidal cells.

Morphological reconstruction and analysis of the neurobiotin-filled neurons

Intracellular injection of tracer neurobiotin during patch-clamp recording sections allowed us to morphologically identify recorded cells as well as their positions in the slice. Neurolucida-reconstructed cells were then analyzed to investigate differences in morphological characteristics. More importantly, the neurobiotin-injection procedure was critical to confirming the position and morphology of the pyramidal-like neurons (by IR-DIC) in the stratum oriens of *Proechimys*. As illustrated in Fig. 7, neurons recorded in stratum radiatum (CA1 and CA2 areas) of Wistar rats are typical pyramidal cells exhibiting apical and basal dendrites. Neurons recorded in the CA1 and CA2 stratum pyramidale of *Proechimys* rats exhibited the typical pyra-

Table 2. Morphological features of reconstructed neurobiotin-filled neurons in CA1 a CA2 subfield of Wistar versus *Proechimys* G

Morphological features	Wistar		*Proechimys*			Statistic ANOVA	
Area Stratum	CA1 Pyramidale n=6	CA2 Pyramidale n=9	CA1 Pyramidale n=5	CA2 Pyramidale n=11	CA1 and CA2 Oriens n=8	F	P-level
Soma							
Area (μm^2)	195.2±14.3	158.2±14.2	112.1±15.4	114.8±9.8	126.9±9.4	6.54	0.0004
Perimeter (μm)	53.7±2.60	47.5±2.07	36.4±3.81	40.1±1.67	42.4±1.55	7.76	0.0001
Dendrites							
Quantity	5.5±0.67	4.4±0.53	3.8±0.58	3.1±0.29	6.2±0.77	5.28	0.002
Nodes	36.17±6.30	24.67±4.39	24.20±8.57	22.09±5.84	32.75±4.96	1.03	0.403
Ends	43.00±5.71	29.33±4.41	27.80±8.61	25.55±5.82	39.75±5.66	1.64	0.186
Mean length (μm)	650.2±168.4	625.5±93.13	508.8±139.9	665.7±178.8	693.9±110.5	0.16	0.953
Total length (μm)	3058±537.9	2530±330.1	1816±543.2	1925±527.8	4274±855.9	2.83	0.039

Data represented as mean±standard deviation. Statistical analysis by ANOVA, significance set at $P<0.05$.

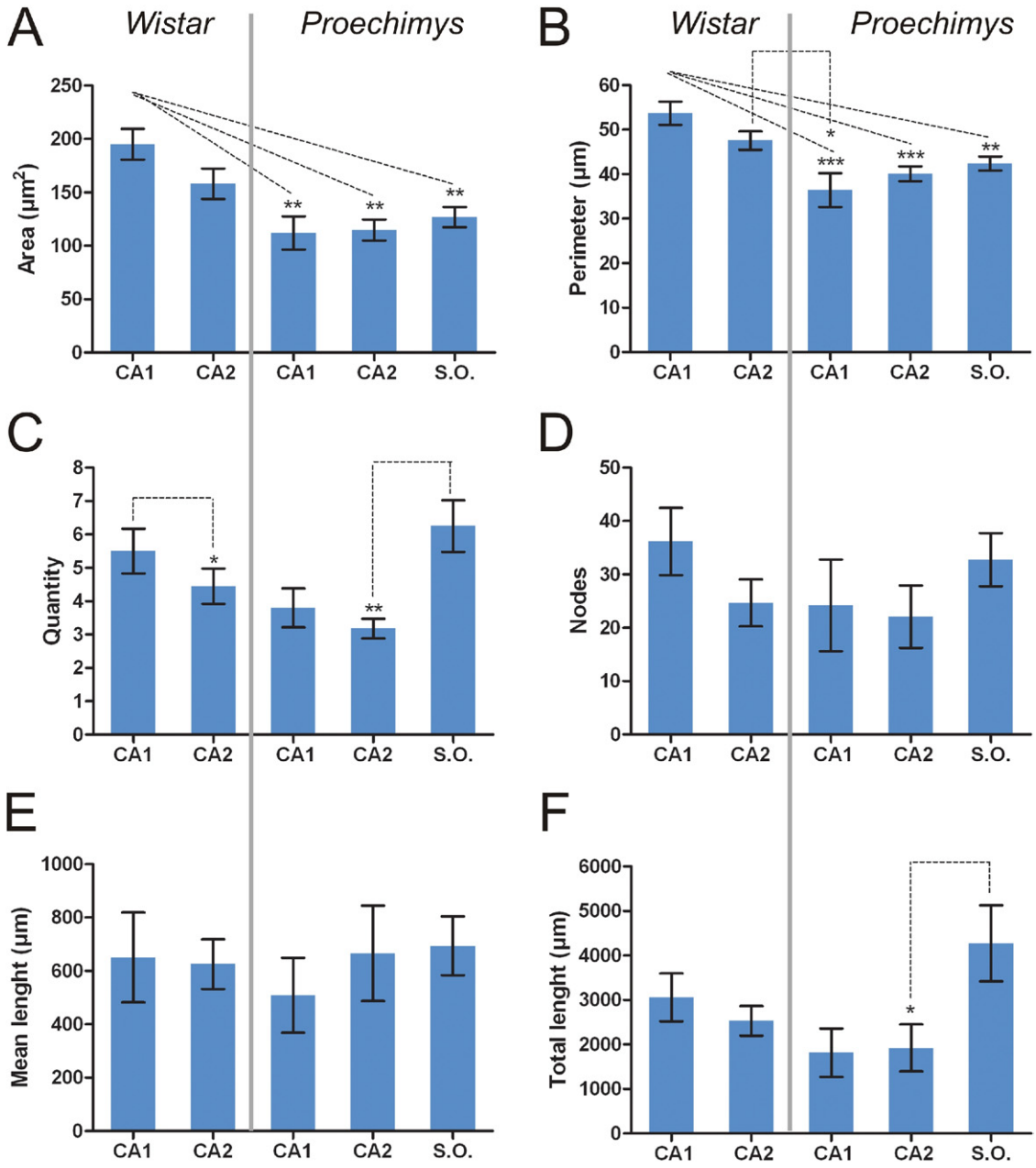

Fig. 12. (A–F) Graphs representing statistical analysis of morphological variables in neurobiotin-filled neurons of Wistar versus *Proechimys* using post-hoc Tukey's HSD test in data sets that were significantly different by one-way ANOVA. * $P<0.05$, ** $P<0.01$, *** $P<0.001$. For interpretation of the references to color in this figure legend, the reader is referred to the Web version of this article.

midal cell morphological phenotype but apparently with less complexity than corresponding neurons in Wistar rats (Fig. 8). Moreover, the reconstruction of the neurons recorded in stratum oriens revealed that the majority of these neurons exhibit a pyramidal cell phenotype with complex apical and basal dendrites (Figs. 9–11). The apical dendrite runs deep into the stratum radiatum of the hippocampus crossing in most cases of the pyramidal layer.

The axon was not consistently labeled in the Neurobiotin-filled neurons. Therefore, we restricted our analysis to morphometric variables of soma and dendrites. ANOVA analysis revealed significant difference in area, perimeter, dendrite number (quantity), and total length among the different experimental groups (Table 2). The area and perimeter of the soma reconstructed neurons in the CA1 subfield of Wistar rats were significantly higher than in *Proechimys* (42% increase in mean area and 31% increase in mean perimeter, $P<0.001$, Table 2, Fig. 12). Pairwise comparisons revealed no significant difference on these variables between CA1 and CA2 pyramidal neurons in Wistar rats. In addition, no significant differences were also observed among pyramidal neurons in *Proechimys*. One-way ANOVA revealed a significant difference among the groups in the quantity of dendrites ($F=5.28$, $P<0.005$,

Table 2). Pairwise comparisons indicate that the number of dendrites was significantly higher in CA1 (20% increase) when compared to CA2 pyramidal neurons in Wistar rats (Post-hoc Tukey's HSD, $P<0.05$) but no significant differences were revealed on the dendrite quantity between Wistar's CA1 and CA2 pyramidal layer neurons when compared to *Proechimys*'s pyramidal layer neurons. A two-fold significant increase in the number of dendrites was noticed in pyramidal-shaped neurons of stratum oriens (CA1 and CA2) of *Proechimys* when compared to CA2 pyramids (post-hoc Tukey's HSD test, $P<0.05$ Fig. 12). No significant difference was revealed in pairwise comparison with CA1 pyramidal layer neurons. Moreover, there were no significant differences between pyramidal neurons in the pyramidal layer of CA1 and CA2 subfield (post-hoc Tukey's HSD, $P>0.05$).

Moreover, the analysis of these morphological variables of neurons in the CA2 area revealed that the perimeter of cells in Wistar rats was 21% larger (Student *t*-test, $P<0.05$) when compared to neurons in *Proechimys* (Table 2). In *Proechimys*, the soma area and perimeter of pyramidal-shaped neurons recorded in stratum oriens were significantly larger than regular pyramidal neurons recorded in the pyramidal layer of CA1 and CA2 areas (Table 2). Moreover, these pyramidal-like neurons exhibited an apparent increase in dendritic arborization with more dendrites (quantity) than neurons in the pyramidal layer of Wistar (increases of 112% in CA1 and 140% in CA2) and *Proechimys* (increases of 163% in CA1 and 200% in CA2). Moreover, these neurons exhibited a larger total length in dendritic arborizations. As observed in Table 2, no significant changes were noticed for the other morphological variables. Overall, these neurons were more morphologically complex as shown in Sholl's analysis (Fig. 13).

Cresyl Violet staining of histological coronal sections containing hippocampus revealed numerous neurons distributed along the stratum oriens of *Proechimys*, confirming our observations using IR/DIC during visualized patch-clamp recordings (Fig. 14). As noticed in sections from Wistar rats, the stratum radiatum has scattered cells with soma oriented in different directions (Fig. 14A, B). These cells are considered to be inhibitory GABAergic neurons; in contrast, the abundant number of pyramidal-shaped cells in the stratum oriens of *Proechimys* indicates that this species has a histologically distinct hippocampus. The origin and role of the pyramidal-like cells has yet to be established. Moreover, an immunofluorescence assay using antibodies against a neurofilament SMI311, which preferentially labels pyramidal neurons in the cortex and hippocampus, showed numerous SMI311-positive neurons located in the stratum oriens of *Proechimys*. Contrastingly, very few SMI311-labeled neurons were present in the stratum oriens of Wistar (Fig. 15A–C). In *Proechimys*'s hippocampus, SMI311 immunostaining was abundant not only in soma and apical dendrites of neurons in stratum pyramidale but also in numerous cells scattered throughout the stratum oriens (s.o.) (Fig. 15D–F). The staining was prominent in soma and apical dendrites of these neurons.

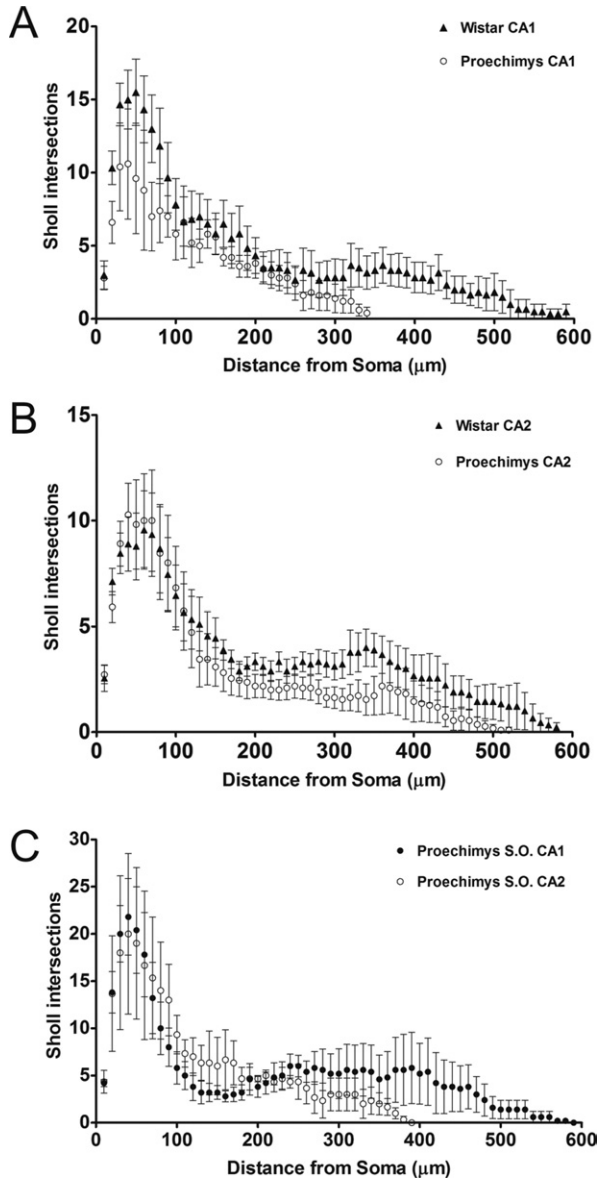

Fig. 13. Sholl's analysis of dendritic arborizations. (A) Sholl analysis comparisons of pyramidal neurons in the stratum pyramidale of CA1 of Wistar versus *Proechimys*. (B) Comparisons of pyramidal neurons in the stratum pyramidale of CA2 of Wistar versus *Proechimys*. (C) Comparisons of pyramidal neurons in the stratum oriens (s.o.) of CA1 and CA2 areas in *Proechimys*. Notice that pyramidal-shaped neurons in stratum oriens of *Proechimys* exhibited a higher complexity, specifically in proximal dendrites (<100 μm from soma) when compared to pyramidal neurons in CA1 (A) and CA2 (B).

A subset of neurons in stratum oriens was devoid of SMI311 immunofluorescence which probably represents the subpopulation of interneurons which are typically distributed in this layer in rodent's hipppocampus (Fig. 15F1, F2, arrows). A higher magnification images of neurons of boxes F1 and F2 in Fig. 15C revealed that some SMI311-positive neurons (soma and apical dendrites) in stratum oriens are surrounded by stronger VGluT1-positive immunolabeling, which may represent excitatory gluatamatergic inputs (Fig. 15F1, F2, arrow heads).

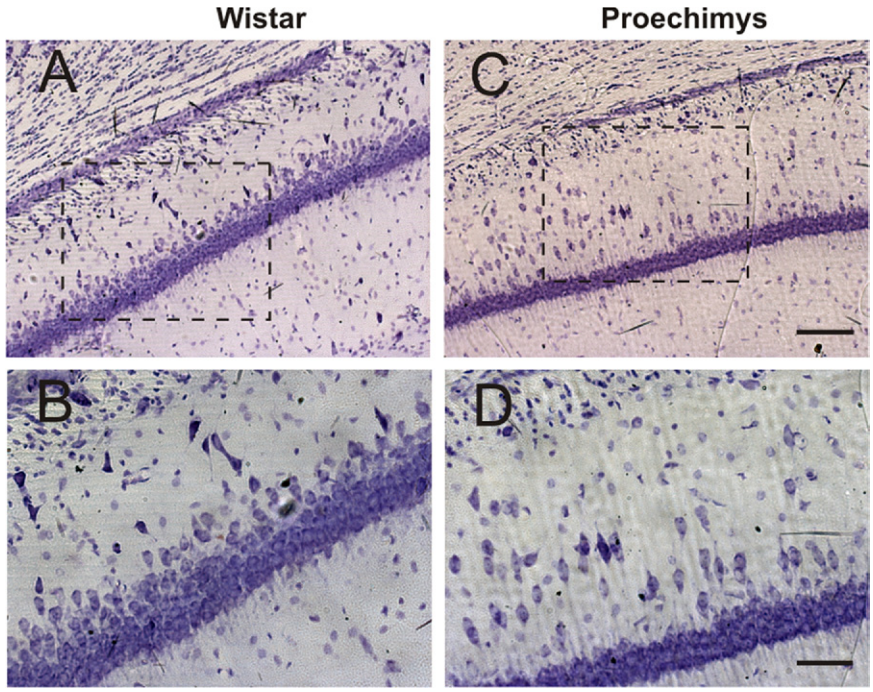

Fig. 14. Nissl staining in the hippocampal area CA1 of Wistar versus *Proechimys*. (A) Representative Nissl staining of the CA1 hippocampal area in Wistar rat. (B) Higher magnification of box showing different morphologies of neurons in stratum oriens (s.o.). (C) Nissl staining of CA1 hippocampal area in *Proechimys*. Notice the presence of numerous neurons oriented in parallel to apical dendrites of pyramidal layer neurons. (D) Higher magnification of area in box showing a group of pyramidal-like neurons in the stratum oriens. Scale in (C)=400 μm and (D)=100 μm. For interpretation of the references to color in this figure legend, the reader is referred to the Web version of this article.

DISCUSSION

In this manuscript, we have described the intrinsic membrane properties and morphological characteristics of CA1 and CA2 pyramidal layer neurons of the *Proechimys*. In addition, by chance, we discovered that pyramidal neurons are scattered through the stratum oriens in this species. Moreover, by performing stimulation of the Schaffer's collateral pathway, it was determined that these neurons receive excitatory inputs from CA3 neurons or locally, most probably from CA1 pyramidal neurons. Hence, these pyramidal neurons in stratum oriens are an integral part of the hippocampal network in this species. These findings provide new direction for the potential use of *Proechimys* in the field of neuroscience. Furthermore, they have direct implications for the study of the normal brain (i.e. synaptic plasticity, cognitive functions, and behavior) as well as for elucidating intrinsic mechanisms of central nervous system disorders.

The analysis of intrinsic properties indicates that pyramidal cell neurons in CA1 and CA2 areas share high electrophysiological homology in Wistar and *Proechimys*. Nonetheless, the newly described pyramidal-shaped neurons in stratum oriens of *Proechimys* exhibited distinctive characteristics. These included larger capacitance, lower input resistance, larger rheobase (it required higher depolarizing current injections to trigger the firing of action potentials), long latency to first action potential, and slower firing frequency. In summary, these cells exhibited lower excitability than the regular pyramidal neurons in CA1 and CA2 area. It is unclear how reduced excitability of these neurons may relate to higher resistance of these animals to develop chronic epileptogenesis. The larger capacitance correlates with the more complex morphological features of these pyramidal-like neurons as observed in the Sholl's analysis and the number and total length of dendrites.

Proechimys is a rodent species living in the Amazonian region that has been recently studied as an animal model of resistance to epilepsy (de Amorim Carvalho et al., 2003). However, the existence of natural endogenous anti-epileptogenic mechanisms remains to be elucidated. Furthermore, previous data of our laboratory also showed a remarkably different *Proechimys*'s cytoarchitecture organization of the hippocampal CA2 subfield (Scorza et al., 2010). In addition to the distinguishing characteristics of the *Proechimys* described so far, our present findings indicated the presence of numerous pyramidal cells in stratum oriens that receive excitatory inputs from CA3 and probably CA1 pyramidal neurons. Assuming that most of the pyramidal neurons throughout the cortex and hippocampus are glutamatergic, we are tempted to speculate that these neurons are also excitatory (i.e. glutamatergic). Another possibility is that these neurons provide strong feedforward excitation of stratum oriens inhibitory interneurons in such a way that the predominant effect may result in an increased inhibition of hippocampal networks. Nonetheless, additional studies are necessary to support such hypothesis. Further studies on the

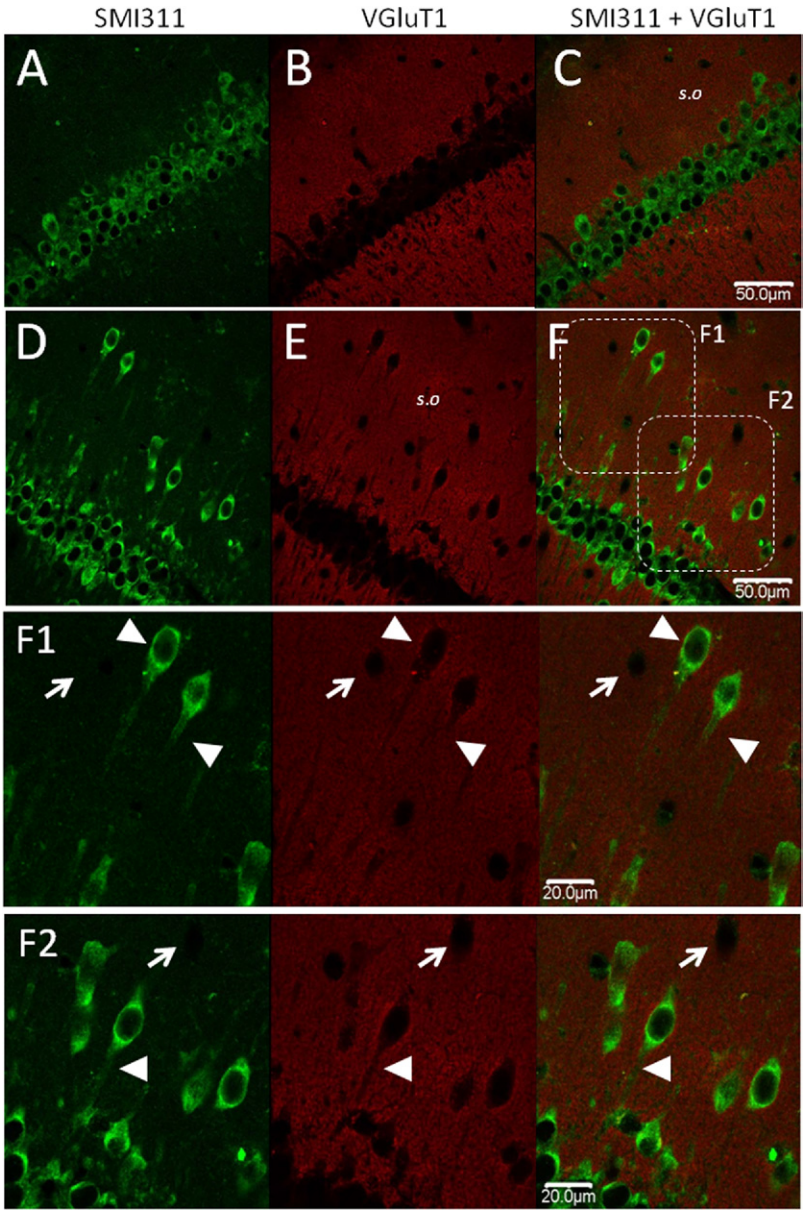

Fig. 15. Representative images from immunofluorescence to detect neurofilament SMI311 (marker of pyramidal neurons) and vesicular glutamate transporter type 1 (VGluT1) in hippocampus of Wistar (A–C) versus *Proechimys* (D–F). SMI311 preferentially labeled soma and apical dendrites of neurons in the pyramidal layer (A, D). Notice numerous SMI311-positive neurons in stratum oriens of *Proechimys*. Immunofluorescence for VGluT1 revealed several immunonegative spaces in stratum oriens of sections in Wistar (B) and *Proechimys* (E), which may correspond to local interneurons (arrows in F1 and F2). In addition, intense VGluT1 staining was noticed around the soma and proximal segment of apical dendrites (arrowheads) in (F1) and (F2). For interpretation of the references to color in this figure legend, the reader is referred to the Web version of this article.

function of pyramidal-like neurons in the *Proechimys* may provide critical information about the hippocampal functioning and dysfunction in tropical rodents. Indeed, several key questions arise from this study: (1) Which is the advantage (i.e. adaptive behavioral, processing of cognitive mapping, spatial navigation, etc) of this additional group of pyramidal neurons localized in the stratum oriens in the *Proechimys* hippocampal network? (2) Is this a common feature of wild rodents or rodents from a specific habitat? (3) What is the origin of the pyramidal neurons in stratum oriens and their physiological significance? Anyhow, a great deal of the knowledge that has improved our understanding of the brain mechanisms has derived from appropriate animal models and, certainly, *Proechimys* represents an important tool of investigation in neurosciences.

Acknowledgments—This work was supported by FAPESP Grant 07/52916-8 (CInAPCe program) and CNPq, CAPES and INCT-Instituto Nacional de Neurociência Translacional, Brazil. E.R.G.S. was

also supported by P20MD001091 (NIH/NCMHD), 5SC1NS063950-04 (NIH/NIGMS/MBRS) and 3SC1NS063950-03S1, USA; M.S.O. was supported by CAPES, Brazil.

REFERENCES

Arida RM, Scorza FA, de Amorim Carvalho R, Cavalheiro EA (2005) *Proechimys guyannensis*: an animal model of resistance to epilepsy. Epilepsia 46 (Suppl 5):189–197.

Davies SN, Collingridge GL (1989) Role of excitatory amino acid receptors in synaptic transmission in area CA1 of rat hippocampus. Proc R Soc Lond B Biol Sci 236:373–384.

de Amorim Carvalho R, Arida RM, Cavalheiro EA (2003) Amygdala kindling in *Proechimys guyannensis* rat: an animal model of resistance to epilepsy. Epilepsia 44:165–170.

Debanne D, Guerineau NC, Gahwiler BH, Thompson SM (1996) Paired-pulse facilitation and depression at unitary synapses in rat hippocampus: quantal fluctuation affects subsequent release. J Physiol 491 (Pt 1):163–176.

Ebinger P (1975) Quantitative investigations of visual brain structures in wild and domestic sheep. Anat Embryol (Berl) 146:313–323.

Fabene PF, Correia L, Carvalho RA, Cavalheiro EA, Bentivoglio M (2001) The spiny rat *Proechimys guyannensis* as model of resistance to epilepsy: chemical characterization of hippocampal cell populations and pilocarpine-induced changes. Neuroscience 104:979–1002.

Hawking F, Walker PJ, Worms MJ (1964) New small animals for laboratory experiment, viz: *Herpestes sanguineus* (African black tailed mongoose), host of filarial worm, *Monnigofilaria setariosa*. *Orizomys goeldi*, *Proechimys guyanensis*, from Brazil. *Thamnomys surdaster*, Congo tree rat, host of *Plasmodium berghei*; colonized in laboratory. Trop Med Hyg 58:292.

Kruska D (1975a) [Comparative quantitative study on brains of wild and laboratory rats. I. Comparison of volume of total brain and classical brain parts]. J Hirnforsch 16:469–483.

Kruska D (1975b) [Comparative quantitative study on brains of wild and laboratory rats. II. Comparison of size of allocortical brain centers]. J Hirnforsch 16:485–496.

Kruska D, Schott U (1977) [Comparative-quantitative investigations of brains of wild and laboratory rats]. J Hirnforsch 18:59–67.

Kruska DC (2005) On the evolutionary significance of encephalization in some eutherian mammals: effects of adaptive radiation, domestication, and feralization. Brain Behav Evol 65:73–108.

Rehkamper G, Kart E, Frahm HD, Werner CW (2003) Discontinuous variability of brain composition among domestic chicken breeds. Brain Behav Evol 61:59–69.

Rohrs M, Ebinger P (1999) [Wild is not really wild: brain weight of wild domestic mammals]. Berl Munch Tierarztl Wochenschr 112:234–238.

Sanabria ER, Silva AV, Spreafico R, Cavalheiro EA (2002) Damage, reorganization, and abnormal neocortical hyperexcitability in the pilocarpine model of temporal lobe epilepsy. Epilepsia 43 (Suppl 5):96–106.

Scorza CA, Araujo BH, Arida RM, Scorza FA, Torres LB, Amorim HA, Cavalheiro EA (2010) Distinctive hippocampal CA2 subfield of the Amazon rodent *Proechimys*. Neuroscience 169:965–973.

Shetty AK, Turner DA (1995) Non-phosphorylated neurofilament protein immunoreactivity in adult and developing rat hippocampus: specificity and application in grafting studies. Brain Res 676: 293–306.

Stricker C, Field AC, Redman SJ (1996) Changes in quantal parameters of EPSCs in rat CA1 neurones *in vitro* after the induction of long-term potentiation. J Physiol 490 (Pt 2):443–454.

Stuermer IW, Wetzel W (2006) Early experience and domestication affect auditory discrimination learning, open field behaviour and brain size in wild Mongolian gerbils and domesticated laboratory gerbils (*Meriones unguiculatus* forma domestica). Behav Brain Res 173:11–21.

(Accepted 27 December 2010)
(Available online 6 January 2011)